8

Diamond as Functional Material for Bioelectronics and Biotechnology

Bohuslav Rezek[1], Marie Krátká[1], Egor Ukraintsev[1], Oleg Babchenko[1], Alexander Kromka[1], Antonín Brož[2] and Marie Kalbacova[2]
[1]*Institute of Physics, Academy of Sciences of the Czech Republic, Prague*
[2]*Institute of Inherited Metabolic Diseases, First Faculty of Medicine, Charles University and General Faculty Hospital in Prague*
Czech Republic

1. Introduction

Understanding the interaction between the biological environment (tissues, cells, proteins, electrolytes, etc.) and a solid surface is crucial for biomedical applications such as bio-sensors, bio-electronics, tissue engineering and the optimization of implant materials. Cells, the cornerstones of living tissue, perceive their surroundings and subsequently modify it by producing extracellular matrix (ECM), which serves as a basis to simplify their adhesion, spreading and differentiation (Shakenraad & Busscher, 1989). This process is considerably complex, flexible and strongly depends on the cell cultivation conditions including the type of the substrate. Surface roughness of the substrate plays an important role (Babchenko et al., 2009; Kalbacova et al., 2009; Kromka et al., 2009; Zhao et al., 2006), other influential factors include both the porosity (Tanaka et al., 2007) and the wettability of the substrate, the latter influencing protein conformation (Browne et al., 2004; Rezek, Ukraintsev, Michalíková, Kromka, Zemek & Kalbacova, 2009) as well as the adsorption and viability of cells (Grausova et al., 2009; Kalbacova, Kalbac, Dunsch, Kromka, Vanecek, Rezek, Hempel & Kmoch, 2007).
Materials which are commonly employed as substrates for in vitro testing are polystyrene and glass. In this context, diamond as a technological material can provide a relatively unique combination of excellent semiconducting, mechanical, chemical as well as biological properties (Nebel et al., 2007). Diamond also meets the basic requirements for large-scale industrial application, most notably, it can be prepared synthetically. Diamond can be synthesized either as a bulk material under high-pressure and high-temperature conditions, or in the form of thin films by chemical vapor deposition of methane and hydrogen on various substrates including glass and metal (Kromka et al., 2008; Potocky et al., 2007). Moreover, the application of selective nucleation makes it possible to directly grow conductive diamond microstructures, which operate e.g. as transistors or pH sensors (Kozak et al., 2010). Nowadays, it is possible to deposit diamond even on large areas (600 cm^2 or more) using linear antennas (Kromka et al., 2011; Tsugawa et al., 2010). The excellent compatibility of diamond with biological materials and environment (Bajaj et al., 2007; Grausova et al., 2009;

Kalbacova, Kalbac, Dunsch, Kromka, Vanecek, Rezek, Hempel & Kmoch, 2007; Tang et al., 1995) is of immense importance for its application in medicine. This bio-compatibility stems from the fact that diamond is a crystalline form of carbon that is mechanically, chemically and physically very stable. Despite the general chemical stability, diamond surface can be terminated by different atomic species (Rezek et al., 2003) and organic molecules (Rezek, Shin, Uetsuka & Nebel, 2007), which can alter diamond's natural properties and thus open the door for countless new applications.

For example, electrical conductance and electron affinity are both significantly influenced by surface termination of diamond by hydrogen or oxygen atoms (Chakrapani et al., 2007; Kawarada, 1996; Maier et al., 2001; Rezek et al., 2003; Ri et al., 1995). The main difference arises from the opposite dipoles of C–H and C–O bonds. Oxygen-terminated diamond is insulating, whereas the hydrogen-terminated surface causes the emergence of two-dimensional hole surface conductance on otherwise insulating diamond. These properties can be exploited for the fabrication of a planar field-effect transistor (FET), whose gate is formed solely by hydrogen surface atoms without the employment of any other insulating layers and which is sensitive to the pH of a solution (Dankerl et al., 2007; Nebel et al., 2006; Rezek, Shin, Watanabe & Nebel, 2007). The hydrogen-terminated diamond surface is also an ideal starting point for covalent bonding of other molecules such as DNA or proteins (Härtl et al., 2004; Rezek, Shin, Uetsuka & Nebel, 2007; Yang et al., 2002). On the other hand, the hydrogen-terminated diamond surface is generally less favorable for the adhesion, spreading and viability of cells than the oxidized surface (Kalbacova, Kalbac, Dunsch, Kromka, Vanecek, Rezek, Hempel & Kmoch, 2007). This difference is due to the hydrophillicity of oxygen-terminated diamond (O-diamond) in contrast to the hydrophobicity of the hydrogen-terminated diamond (H-diamond). As a result, the combination of both hydrogen- and oxygen-terminated diamond surface is very interesting for bio-electronics (Dankerl et al., 2009; Rezek, Krátká, Kromka & Kalbacova, 2010) as well as for tissue engineering (Kalbacova et al., 2008; Rezek, Michalíková, Ukraintsev, Kromka & Kalbacova, 2009).

In this chapter we present the influence of micro-structuring morphology and atomic termination of diamond surfaces on cell growth and assembly. We investigate the influence of key parameters such as the seeding concentration of cells, the type of the applied cells, the duration of cultivation, the concentration of fetal bovine serum (FBS) in the cultivation medium, the dimensions and shape of microstructures, and surface roughness. We show that the adsorption of proteins from the FBS serum is the key factor. Atomic force microscopy (AFM) both in solution and in air is applied in order to characterize the morphology of the FBS layers adsorbed on differently terminated diamond substrates. The influence of proteins and cells on the electronic properties of diamond is demonstrated by employing a field-effect transistor on hydrogen-terminated diamond, whose gate is exposed to a solution (SG-FET). These results are discussed from the point of view of fundamental physics and biology as well as the prospects in medicine.

2. Preparation of nanocrystalline diamond layers

The growth of thin-film nanocrystalline-diamond layers (NCD) was realized on silicon or glass substrates using microwave plasma enhanced chemical vapor deposition (MW-CVD) (Kromka et al., 2008; Potocky et al., 2007). The substrates were 10×10 mm^2 large and had

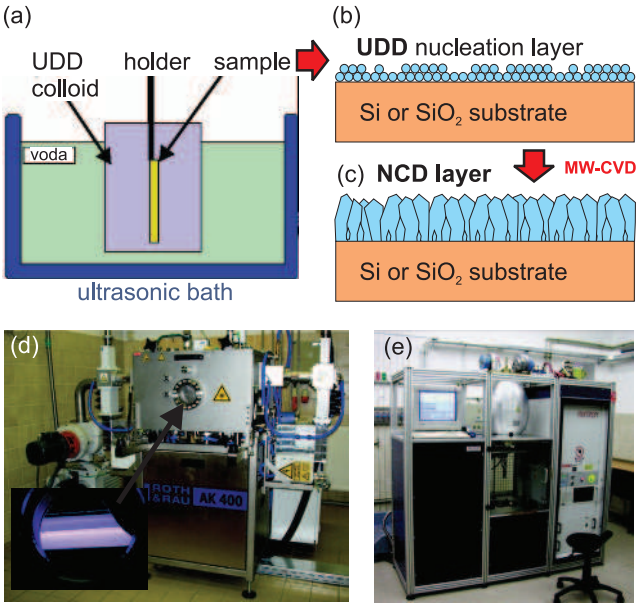

Fig. 1. Schematic depiction of the preparation procedure of thin-film diamond on glass or silicon substrates: (a) nucleation of the substrates carried out in an ultrasonic bath with ultra-dispersed diamond (UDD), (b) the resulting nucleation layer and (c) the nanocrystalline diamond layer after the microwave-plasma deposition. The deposition machines for (d) large-area growth of diamond (linear plasma) and (e) high-speed growth (focused plasma).

surface roughness < 1 nm. Before the deposition, the substrates were ultrasonically cleaned in isopropanol and deionized water and were subsequently immersed for 40 min into an ultrasonic bath with a colloidal suspension of a diamond powder (UDD – ultra-dispersed diamond; NanoAmando, New Metals and Chemicals Corp. Ltd., Kyobashi) with nominal particle size of 5 nm. This process leads to the formation of a 5- to 25-nm-thin layer of nanodiamond powder. This nucleation procedure was followed by a microwave plasma-enhanced chemical vapor deposition (MW-CVD) of diamond films. The deposition conditions were: temperature of substrates 600–800°C, 1% CH_4 in H_2, microwave power 1.4–2.5 kW, gas pressure 30–50 mbar, duration approximately 4 hours, the thickness of layers reaches 100–500 nm. The same conditions, only with methane gas switched off and process time 10 min, were used for H-termination of the diamond surface. In some cases, the nucleation and growth were repeated on the other side of the substrate, which leads to the hermetical encapsulation of the substrate by the NCD layer (Kalbacova et al., 2008; Rezek, Michalíková, Ukraintsev, Kromka & Kalbacova, 2009). The preparation procedure is schematically shown in Figure 1. This figure also depicts the photos of the set-ups for the large-area diamond growth (linear plasma) with high deposition rate (focused plasma).
NCD layer were chemically cleaned in acids (97.5% H_2SO_4 + 99% KNO_3 powder in the ratio of 4:1) at 200°C for 30 minutes. This process ensures high quality of the hydrogen-terminated surface (surface conductance in the order of 10^{-7} S/sq) (Kozak et al., 2009). The surface morphology and chemical quality of NCD layers were characterized by AFM, scanning

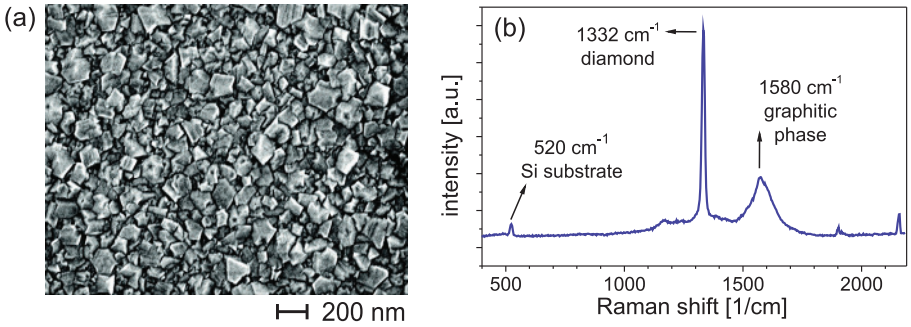

Fig. 2. Basic characteristics of a typical NCD layer on Si: (a) morphology by SEM and (b) a typical Raman-scattering spectrum.

electron microscopy (SEM) and Raman spectroscopy. Roughness evaluated in the tapping AFM regime is 15 – 30 nm rms (1×1 μm^2 area), grain size as measured by SEM is 50 – 150 nm (see Figure 2(a)). The grains exhibit clear facets that evidences their crystalline diamond form. Raman spectroscopy (excitation wavelength 325 nm) confirmed the diamond character of the layers (see Figure 2(b)). With a small alteration of the deposition conditions, grain sizes of even several hundreds of nanometers can be reached.

3. Cell growth on diamond with surface nanostructures

To produce nanostructured diamond surfaces the NCD films were first masked with: i) 5 nm diamond nanoparticles using the ultrasonic treatment in UDD colloidal suspension, ii) 30 nm nickel particles prepared by deposition of 3 nm nickel layer on diamond and its treatment in hydrogen plasma for 5 min (Babchenko et al., 2009). Subsequent etching of diamond nanostructures was performed by reactive ion etching (RIE) system (Phantom LT RIE System, Trion Technology) at about 100°C for 300 s using 2 sccm of CF_4 and 50 sscm of O_2. Remaining nickel masks were then removed by a wet etching process. Finally, the diamond surfaces were treated in r.f. oxygen plasma to obtain hydrophilic character of the surface that is suitable for cellular adhesion (Kalbacova, Kalbac, Dunsch, Kromka, Vanecek, Rezek, Hempel & Kmoch, 2007).

Scanning electron microscopy (SEM) images of the NCD films with nanoparticle masks and after the RIE process are shown in Figure 3a-b and 3e-f. Diamond nanoparticle mask resulted in a formation of isolated cone-like structures (height 5–100 nm, diameter up to 80 nm) randomly spread on the remaining NCD film. Mask made of the nickel nanoparticles resulted in a formation of upright, densely packed diamond nanorods with the height of 120–200 nm and diameter 20–40 nm. Diamond nanoparticles are obviously (and expectably) not enough resistant to the plasma etching process. Therefore, the surface exhibit lower density of cone-like structures. Nickel nanoparticles were able to withstand the whole etching period, hence the nanorods were formed.

These nanostructured diamond surfaces were used as artificial substrates for growth of human osteoblast-like cells. Human osteoblast-like cells (SAOS-2; DSMZ, Germany) were plated on the samples in 25,000 cells/cm^2 concentration and grown in the McCoy's 5A medium without phenol red (BioConcept) supplemented with 15% heat-inactivated fetal

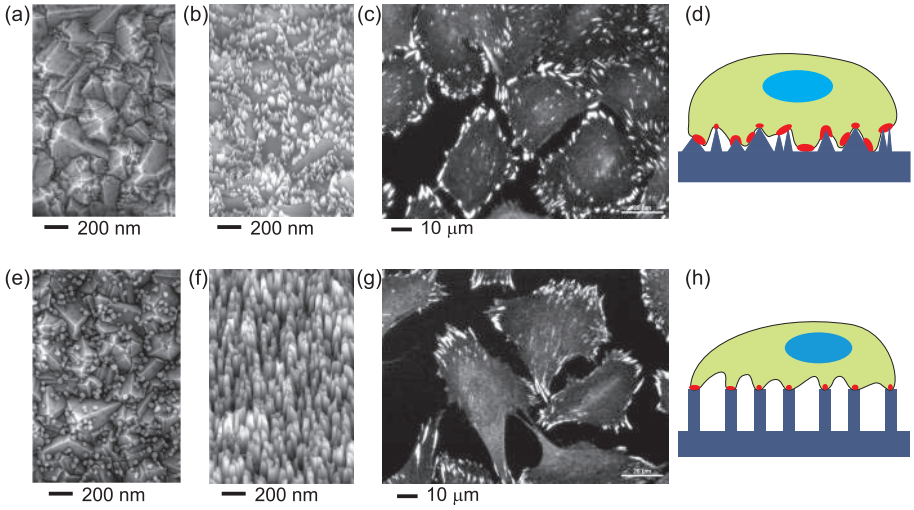

Fig. 3. Scanning electron microscopy (SEM) image of the NCD layer (a) with diamond nanoparticle mask and (b) resulting nanostructured surface (nano-cones) after plasma etching. (c) Fluorescence microscopy image of stained focal adhesions (vinculin) of osteoblast-like cells on the surface with nano-cones. (d) Schematic drawing of cellular adhesion on the nano-cones (focal adhesions – red, nucleus – blue, cytoskeleton – green). Same measurements for the case on nickel nanoparticle mask and diamond nanorods are shown in (e-h).

bovine serum (PAA), 20 U penicillin and 20 μg/ml streptomycin in a humidified 5% CO_2 atmosphere at 37°C. Resulting morphology of focal adhesions of SAOS-2 cells was characterized by immunofluorescent staining of vinculin (1:150, Sigma, anti-mouse Alexa 568) and imaging in the epi-fluorescence microscope (Nikon E-400).
The fluorescence images are shown in Figure 3c and 3g, next to the SEM images. Based on the fluorescence images, osteoblasts exhibit generally well spread fibroblast-like morphology on both substrates. During the 48h incubation the cells went through one cell cycle. This also indicates general substrate suitability. However, the size and shape of highlighted focal adhesions differ on each type of the nanostructures. Osteoblasts cultivated on relatively short and broad nano-cones form well pronounced large focal adhesions with intensive vinculin staining indicating bigger surface available for adhesion and thus stronger adhesion contacts between cell and diamond. On the other hand, cells cultivated on relatively high and thin nanorods form very thin and fine focal adhesions indicating weaker adhesion. This is schematically shown in Figure 3d and 3h. Another crucial role in cell-diamond interaction play atoms terminating the diamond surface.

4. Cell growth on diamond with atomic micro-patterns

To characterize influence of diamond surface atoms on the arrangement of cells, NCD layers with hydrogen and oxygen surface atoms forming microscopic patterns of widths from 30 to 200 μm were fabricated as follows. Positive photoresist ma-P1215 (micro resist technology GmbH, Germany) was spin-coated on the NCD surface an micro-patterned by

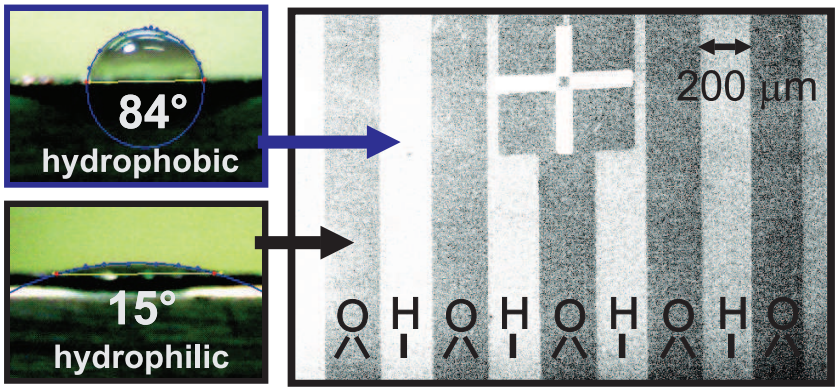

Fig. 4. SEM image of a nanocrystalline-diamond layer with 200-µm-wide stripes with alternating hydrogen and oxygen termination. Light stripes correspond to the hydrogen surface due to its low electron affinity. The cross in the upper part of the image is made up of a thin layer of gold and serves as a mark for the differentiation of particular stripes. Typical measurements of wetting angle on the two types of diamond surfaces (uniformly terminated) are shown along the left side of the SEM image.

optical lithography. Afterwards, the NCD layers were exposed with a photolithographic mask in high-frequency oxygen plasma (power 300 W, duration 3 minutes), which gives rise to the oxidation of the surface, and, consequently, to the formation of hydrophilic patterns. The wetting angle of water on oxygen-terminated diamond was $< 20^{\circ}$, in contrast to about 80° on the hydrogen-terminated diamond. The morphology of the surface remains unchanged during this procedure. Figure 4 shows how the microscopic stripe patterns look look like in an electron microscope (hydrogen and oxygen stripes have different SEM contrast due to different electron affinity).

Before cell plating, the NCD layers were sterilized using either UV irradiation or 70% ethanol treatment for 10 minutes. In most experiments, the cell line of human bone cells (osteoblasts – SAOS-2 cells; DSMZ GmbH) were used. The cells were plated on diamond in the concentrations ranging from 2,500 (sub-confluent coverage) to 10,000 cells/cm^2 (confluent coverage, when the cells are in direct contact with each other) and immersed in the McCoy's 5A (BioConcept) medium, which contains penicillin (20 U/ml) and streptomycin (20 μg/ml) and different concentrations of FBS (0–15%). Then, the cells were cultivated in an incubator at 37°C in 5% CO_2 for 48h. We used osteoblasts because SAOS-2 is a standard cell line, whose properties are stable even for long timespans. This is why we are able to compare the results of different experiments, as well as our results with the literature. Other cell types were also applied for comparison: human periodontal ligament fibroblasts (HPdLF; Lonza) and human cervical carcinoma cells (HeLaG; DSMZ GmbH).

Adhesion and morphology of cells were characterized by fluorescent staining of actin stress fibers (in green) and cell nuclei (in blue) using the protocol described in (Kalbacova, Roessler, Hempel, Tsaryk, Peters, Scharnweber, Kirkpatrick & Dieter, 2007). The staining was visualized using the E-400 epifluorescence microscope (Nikon); digital images were acquired with a DS-5M-U1 Color Digital Camera (Nikon).

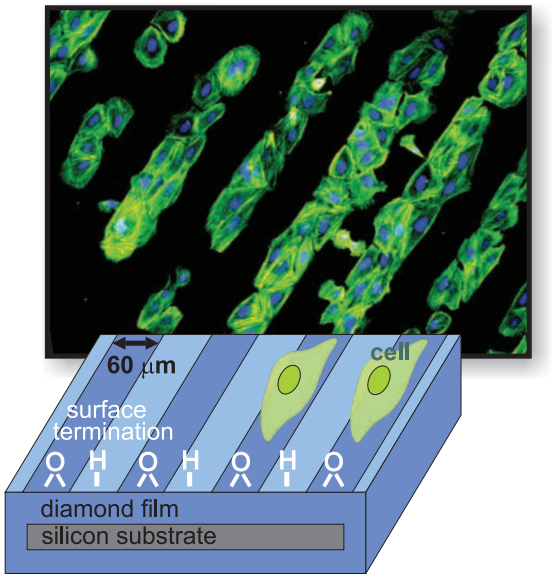

Fig. 5. Microscopic fluorescence image illustrates how osteoblastic cells (SAOS-2) preferentially self-assemble on oxygen-terminated diamond after a 48h cultivation in McCoy's 5A medium with 15% FBS on H-/O-diamond stripes of 60 μm width. Starting cell concentration was 2,500 cells/cm^2. Fluorescence microscopy shows actin filaments in green and cell nuclei in blue. The scheme under the image further clarifies the situation.

When the osteoblastic cells were plated and grown on the H-/O-terminated microstructures, they self-assembled preferably on the oxygen-terminated diamond surface. A scheme and fluorescence image shown in Figure 5 give an example of such behavior for the case of 60-μm-wide stripes. The cells' preference is independent of the width of the stripes between 30 and 200 μm (Rezek, Michalíková, Ukraintsev, Kromka & Kalbacova, 2009) and of the surface roughness between 20 and 500 nm rms (Michalíková et al., 2009). However, the shape of cells was found to be influenced by surface roughness (Kalbacova et al., 2009; Kromka et al., 2009) and the width of microstructures (Kalbacova et al., 2008; Rezek, Michalíková, Ukraintsev, Kromka & Kalbacova, 2009). Cells grown on narrow O-stripes (30 μm i.e. comparable with the size of the cell) are elongated and form chain-like structures. On the other hand, cells growing on wider stripes (60, 100 a 200 μm – larger than the typical cell size) spread over the whole width of the stripe. The H-/O-diamond boundary forms a sharp interface for cell adhesion.

Figure 6 confirms that other types of cells are also able of controlled self-assembly on H-/O-diamond stripes. Human fibroblasts (HPdLF) and cervical carcinoma cells (HeLaG) were plated on NCD samples with 30-μm-wide stripes and were cultivated for 48h. Cells exhibit a different morphology, however, their preference for O-diamond remains unchanged. Selective growth of cells on H-/O-diamond is also influenced by the seeding concentration, which is illustrated in Figure 7. At low concentrations (2,500 cells/cm^2), the cells grow predominantly on the oxygen-terminated surface, where the cells have enough room to

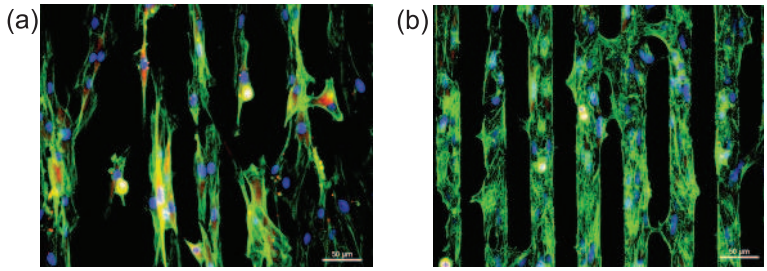

Fig. 6. Fluorescence image of (a) fibroblasts (HPdLF) and (b) cervical-carcinoma cells (HeLaG), which were cultivated for 48h on 30-µm-wide H-/O-diamond stripes. Starting cell concentration was 2,500 cells/cm^2, medium was supplemented with 15% FBS. Fluorescence microscopy shows actin filaments in green and cell nuclei in blue.

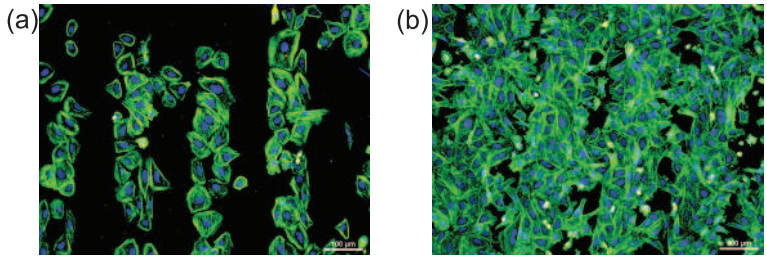

Fig. 7. Fluorescence images of osteoblasts, which were cultivated for 48h on 100-µm-wide H-/O-diamond stripes with starting cell concentrations: (a) 2,500 cells/cm^2, (a) 10,500 cells/cm^2. Fluorescence microscopy shows actin filaments in green and cell nuclei in blue.

spread on a hydrophilic area (Figure 7(a)). On the other hand, cells plated at high seeding concentrations (10,000 cells/cm^2) colonize also the hydrogen-terminated surface (Figure 7(b)). The FBS serum is another factor which has impact on the selective growth of cells. Figure 8 depicts the influence of FBS in the cultivation medium on the arrangement of cells on the H-/O-diamond terminated stripes. The range of concentrations between 5% and 15% does not significantly influence the cell adhesion (image for 15% FBS concentration is shown). Nevertheless, cells plated in a medium without FBS assemble of the surface independently of the surface termination. The cells' preference for a particular type of surface is thus presumably determined by the FBS proteins and not by a direct interaction between diamond surface dipoles and the cells. This is why the properties of FBS layers adsorbed on different types of diamond surfaces were investigated.

5. Morphology of protein layers on H-/O-diamond

Adsorption, adhesion and conformation of FBS layers on diamond were studied using AFM (Ntegra, NTMDT). The AFM measurements were carried out in air and in solution both in contact and tapping regimes. Doped silicon cantilevers (Multi75Al, BudgetSensors) with typical spring constant of 3 N/m, resonant frequency 75 kHz in air and 30 kHz in solution and nominal tip radius $<$ 10 nm were used. Polished monocrystalline diamond was used as a substrate to minimize the influence of its surface

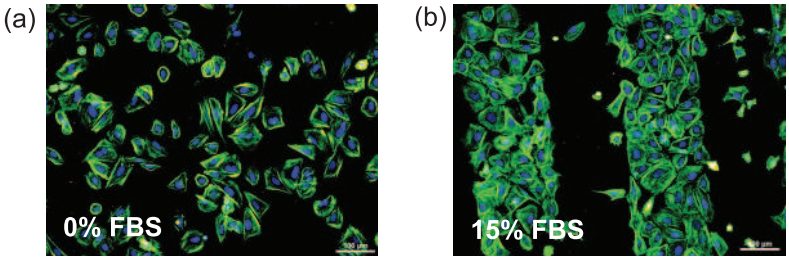

Fig. 8. Fluorescence images of osteoblasts, which were cultivated for 48h on 100-µm-wide H-/O-diamond stripes with different starting concentrations of fetal bovine serum: (a) 0%, (a) 15%. Fluorescence microscopy shows actin filaments in green and cell nuclei in blue. In the 0% case, the cells were plated without the serum, however, the serum was added after 2 hours to allow cells to grow for next 48 h.

morphology on the layers. Surface terminations were prepared in the same way as in the case of NCD films. The thickness of the protein layer was determined using the nanoshaving method, in which a part of the protein layer is removed by means of the AFM tip in contact mode and subsequently the profile of the resulting step in height is measured in oscillating (tapping) mode (Rezek et al., 2006; Rezek, Shin, Uetsuka & Nebel, 2007; Rezek, Ukraintsev, Michalíková, Kromka, Zemek & Kalbacova, 2009). Polished monocrystalline diamond is an ideal substrate for this method, because it is flat and hard.
Proteins were adsorbed on the surface of diamond from 15% FBS solution (Biowest) in McCoy's 5A medium (BioConcept). Two adsorption methods were applied: (i) either a drop of the solution was deposited on the substrate by a pipette, the substrate was then kept in a humid chamber for 10 minutes and was subsequently rinsed with water, or (ii) the adsorption was carried out directly in a fluid cell of AFM microscope with a subsequent *in-situ* measurement. Both methods yielded comparable results. The protein monolayer formed on the diamond surface within several seconds after the application (Rezek, Ukraintsev, Michalíková, Kromka, Zemek & Kalbacova, 2009).
AFM nanoshaving experiments showed that the thickness of the protein layer adsorbed from the solution is (4 ± 2) nm on O-diamond and (1.5 ± 2) nm on H-diamond (Rezek, Ukraintsev, Michalíková, Kromka, Zemek & Kalbacova, 2009). Thus, FBS layers formed on both types of diamond surfaces. Figure 9 presents a detailed topography and a phase map of the protein layers measured in AFM. Standard deviation values (i.e. RMS – root-mean-square) of the height and phase signals together with the characteristic lateral size of the features (L_x) determined by means of the autocorrelation function are shown below the images. In the case of the topography, RMS value corresponds to surface roughness. Roughness of the FBS layer on H-diamond (0.6 nm) is approximately $3\times$ smaller when compared to the O-diamond layer (1.7 nm). Besides, the features on the surface are of different shapes and sizes (12 and 18 nm, respectively). The phase signal exhibits an even more pronounced difference. Whereas in the H-diamond case the phase image of the FBS layer consists of dark dots correlating with the protrusion in topography, the O-diamond phase image is characterized by much larger light areas, which correlates with round structures in topography. In air AFM experiments in air, such differences in topography and phase channel were not observed (Rezek, Ukraintsev, Michalíková, Kromka, Zemek & Kalbacova,

2009). This discrepancy results from the fact that FBS layers are not in their natural environment (solution).

Atomic force spectroscopy then showed that a characteristic sawtooth profile in tip-surface interaction of 500 ± 100 pN force in the adhesion part of the curve (negative force) can be detected (Rezek, Michalíková, Ukraintsev, Kromka & Kalbacova, 2009). Typical curves are shown in Figure 9(e). Similar values of forces and interactions were detected in force curves on glass-adsorbed proteins where they were attributed to the stretching of the proteins by the AFM tip (Popov et al., 2007). The character of the force curves is thus a proof that the FBS proteins are adsorbed on both types of diamond surfaces.

Based on these AFM measurements, we propose a model of the conformation of proteins adsorbed on diamond surfaces (Rezek, Ukraintsev, Michalíková, Kromka, Zemek & Kalbacova, 2009). This model is schematically depicted in Figure 9(f). On hydrophobic surfaces, the denaturation of proteins (i.e. negative conformational change) occurs because their hydrophobic core sticks to the hydrogen-terminated surface. On hydrophilic surfaces, on the other hand, the proteins remain in their natural globular shape. This is why AFM detects a different shape, height and energy dissipation (phase) on the protrusions on the surface. Similar behavior of proteins was observed also on other materials (Browne et al., 2004).

6. Electronic effects on the diamond-protein-cell interface

Hydrogen-terminated stripes surrounded by oxygen-terminated areas were further utilized as conductive channels of *p*-type SG-FET transistors (Rezek, Shin, Watanabe & Nebel, 2007), which serves as a tool for the characterization of the influence of adsorbed proteins and cells grown on them on the electronic properties of diamond (Rezek, Krátká, Kromka & Kalbacova, 2010). The top-view and cross-section diagrams of the SG-FET transistor are shown in Figures 10(a) and 10(b), respectively. Electrical contacts were prepared by the sputtering of thin metal layers (10 nm Ti and 50 nm Au) over a photolithographic mask and the subsequent application of the lift-off technique. The transistor was insulated from the electrolyte using a layer of photoresist (1.5-µm-thick ma-P1315 or 5-µm-thick SU8-3050). Within the active area of the transistor, openings of about 60×60 µm^2 were introduced to this insulating layer. These openings exposed the surface of the 20-µm-wide conductive channel and partly also the surrounding oxidized surface (about 20 µm from each side) (Rezek, Krátká, Kromka & Kalbacova, 2010). The transistor gate was generated by the immersion of this active area in the solution (electrolyte), which is in contact with an Ag/AgCl reference electrode. The gate is insulated solely by hydrogen surface atoms without the employment of any other insulating layers.

Output and transfer SG-FET transistor characteristics were measured using two Keithley K327 source-measure units connected according to Figure 10(a). Characteristics were acquired in the following solutions: (a) McCoy's 5A medium, (b) McCoy's 5A medium with 15% FBS and (c) McCoy's 5A medium with Britton-Robinson buffer at pH = 7. In order to ensure that the acquired characteristics represent stable data, all the measurements were repeated three times. Output characteristics in Figure 10(c) confirms that nanocrystalline-based transistors are fully functional in solution and its behavior under gate voltage is in accord with what is expected for a *p*-type channel. This functionality was reached even in NCD layers as thin as 100 nm with the average grain size of (80 ± 50) nm. The influence of the adsorption of proteins and

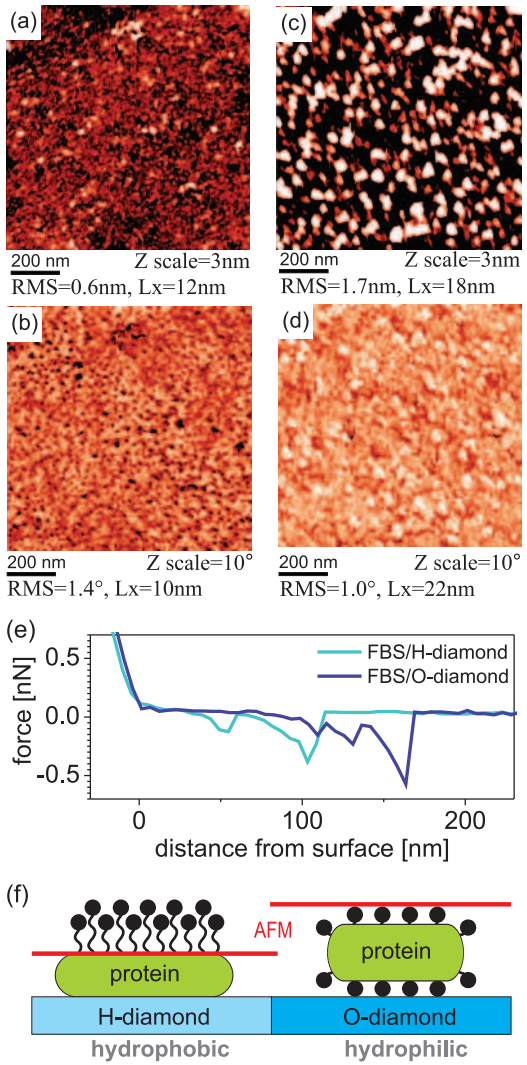

Fig. 9. Atomic force microscopy (AFM) on hydrogen- and oxygen-terminated diamond surfaces with an adsorbed FBS layer in FBS/McCoy's medium: topography and phase (a-b) of FBS/H-diamond, (c-d) FBS/O-diamond. Values of standard deviation (RMS) of the height and phase channel and characteristic lateral size of the features (L_x) below the images were determined using the autocorrelation function. (e) Typical atomic force spectroscopy curves for an FBS layer on hydrogen- and oxygen-terminated diamond surface. (f) Model of the conformation of proteins on hydrogen- and oxygen-terminated diamond surface. Hydrophobic core in green, the black spheres represent polar groups surrounding the core in aqueous environment. The red line denotes the height of the protein as detected by AFM in solution.

subsequent growth of cells on the electronic properties of diamond is easily discernible in Figure 10(c), which represents transfer characteristics of a pristine diamond transistor (blue), the same transistor after the adsorption of FBS (red) and after SAOS-2 cell cultivation (green). All characteristics were acquired in the McCoy's 5A medium, source-drain voltage was kept constant during all the measurements (-0.6 V; this setting corresponds to the amplification regime of the transistor). A slight hysteresis effect was observed in all transfer characteristics. Current flowing through the SG-FET transistor decreased after the application of FBS and the transfer characteristics shifted approximately by -45 mV for $I_{ds} = -0.6$ nA. Another shift roughly by -78 mV was observed after the cultivation of cells, giving rise to an overall shift of about -123 mV. Apart from the shift, the steepness of the slope (transconductance) defined as $g_m = \delta I_{ds}/\delta Ug$ decreased from 9.5 to 8.3 nS at $I_{ds} = -0.6$ nA. Rinsing the sample with the McCoy's medium (Rezek, Krátká, Kromka & Kalbacova, 2010) had only little impact on the characteristics. Transistor gate (leakage) currents were in the order of 10 pA. Typically, FBS adsorption on the surface reduced the gate currents as FBS forms additional layer on the diamond surface. Yet in some cases the currents slightly increased (to about 40 pA) as a result of the adsorption of proteins (Rezek, Krátká, Kromka & Kalbacova, 2010).

7. Discussion

Interaction of cells with as-grown and nanostructured diamond surfaces indicates that the diamond surface morphology can be tailored in a controlled way with respect to bio-technological and bio-medical requirements. It also demonstrates that quite wide range of diamond surface morphologies is acceptable for the cell growth. This is in agreement with other experiments on diamond films where hierarchically modified substrate roughness was employed (Kalbacova et al., 2009).

In the case of nanostructured diamond surfaces, amount of vinculin detected by fluorescence microscopy can be used an indication of the cell motility on the substrate because vinculin generally serves as a stabilizing protein in the focal adhesion (Fernandez et al., 1992). Increased expression of vinculin on the nano-cones promotes the cell adhesion and reduces the cell motility. On the nano-rods, solitary cells have more chance to move and search the entire space, whereas cells in confluent layer could be easily peeled off.

In the case of hydrogen- and oxygen-terminated microstructures, cells preferably self-assemble on the oxygen-terminated surface. The growth of cells over the hydrogen-terminated areas, mostly at high cell concentrations, is presumably enabled by their linkage to the O-diamond layers because individual cells exhibit poor adhesion to H-diamond and reduced metabolic activity (Kalbacova, Kalbac, Dunsch, Kromka, Vanecek, Rezek, Hempel & Kmoch, 2007; Kalbacova et al., 2008). Very probably, cells communicate, exchange growth factors and various stimuli and gradually form the extracellular matrix (ECM). In this way, they modify the surface with proteins and proteoglycans underneath them to overcome the unfavorable properties of the substrate. This process then makes it possible for the cells to grow also over the electrically conductive H-diamond areas, if these are surrounded by O-diamond areas. This effect was exploited during the incubation of cells in field transistors.

Figure 8 clearly demonstrates that the FBS proteins are the factor whose influence determines the cell adhesion on the diamond layer. As the protein adsorption proceeds much more rapidly than the transport of cells to the surface, the interaction of the cell with the diamond

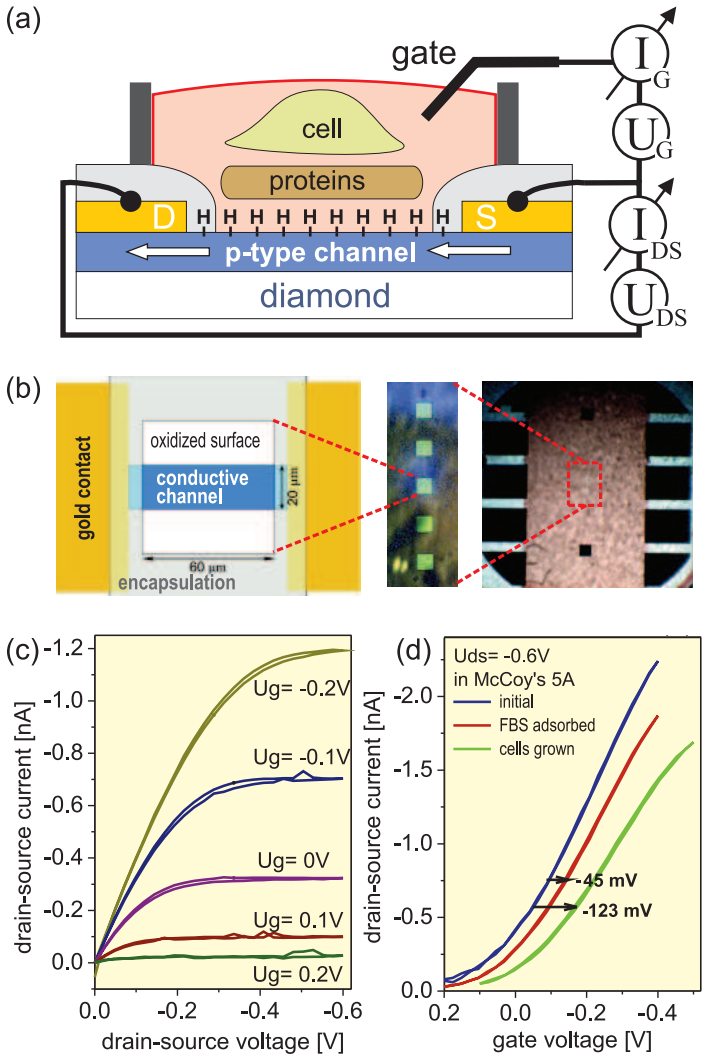

Fig. 10. (a) Diagram of a solution-gate field-effect transistor (SG-FET) based on the surface conductivity of hydrogen-terminated diamond. The insulation of the SG-FET gate is ensured merely by the hydrogen termination of the diamond channel surface. Thus, proteins and cells react directly with the surface of diamond. (b) Top-view: hydrogen-terminated conductive microscopic channel is surrounded by insulating oxygen-terminated areas and the active area is determined by the hole in the insulating layer. A chip contains several such areas, as is demonstrated in the optical image of the whole chip (10×10 mm^2 with 5 transistors) on the right. (c) Output characteristics of SG-FET transistor from nanocrystalline diamond in McCoy's 5A solution with gate potential between -0.2 and 0.2 V. (d) Transfer characteristics of a transistor in McCoy's 5A solution at the beginning of the experiment (blue), after the adsorption of proteins from FBS (red) and after 48h cell cultivation (green)

substrate very likely results from the nature of this adsorbed layer. AFM measurements show that proteins adsorb on both types of surfaces, which agrees well with experiments carried out on other materials, where albumin adsorbs both on hydrophilic and on hydrophobic surfaces (Browne et al., 2004). The selectivity of the cell growth is thus not determined by FBS adsorbing solely on a one type of surface. Other factors, such as denaturation of proteins on hydrophobic surfaces, need to be taken into account in order to successfully explain the selective adsorption. Detailed study of surface morphology using the AFM method clearly confirms that differences in surface roughness, morphology as well as phase contrast between the protein layers on H- and O-diamond exist. When on H-diamond, the FBS proteins probably adopt the conformation when their epitopes (e.g. adhesion mediated RGD sequences of peptides) are hidden, thus not providing optimal conditions for cell adhesion. A similar difference in protein morphology was observed on polystyrene substrates (Browne et al., 2004). This is why the wetting properties of a surface seem to be the most influential factor for the growth of cells, whereas other specific properties of diamond layers do not play such an important role. As we have shown, this phenomenon is general and valid also for other types of cells.

The above described preference of the cells for oxygen-terminated surface on H/O-patterned diamond is detectable as early as during the first two hours of adsorption in the 15% FBS supplemented medium (Rezek, Michalíková, Ukraintsev, Kromka & Kalbacova, 2009). However, the pattern is not yet as sharp as after 48h because the cells did not have enough time to spread on the surface. On the other hand, in a control experiment without FBS the patterned self-assembly was not observed. This implies that even the initial stage of the assembly is strongly influenced by the FBS proteins. In this stage, cells move and actively explore their surrounding environment.

Other factors that can influence the selective cell growth include a different adhesion of cells and proteins to hydrogen- and oxygen-terminated surface. Also a differences in composition of the protein layer on each type of surface can play role. Adhesion of cells to the hydrogen-terminated diamond lowered by as much as 40% was observed in the presence of FBS in comparison to oxygen-terminated diamond (Rezek, Ukraintsev, Kromka, Ledinský, Brož, Nosková, Hartmannová & Kalbacova, 2010). Furthermore, fibronectin, one of the FBS components, was found to have the crucial influence on the selective growth of cells (Rezek, Ukraintsev, Kromka, Ledinský, Brož, Nosková, Hartmannová & Kalbacova, 2010). Detailed composition of the FBS layer on diamond, however, has not yet been successfully identified.

In the medium without FBS, the cells cannot detect any protein layer and thus they are in direct contact with the NCD substrate. After a short time (2 hours), the cells are not yet fully spread, but their contacts (focal complexes) with the substrate are already detectable (Rezek, Michalíková, Ukraintsev, Kromka & Kalbacova, 2009). In general, the adhesion mechanism is not yet understood. After further cultivation time (48 hours) in the medium where FBS was added, the cells assume normal shapes and growth takes place properly at the spots where the cells initially attached (see Figure 8(a)) because they had enough time to produce their own extracellular matrix and adapt the surface underneath them. The hydrogen- or oxygen-termination of diamond (without the initial activity of the FBS proteins) is, therefore, not the sole factor determining the cells selectivity by itself.

From the point of view of electronic properties of the diamond-protein-cell system, SG-FET diamond transistor exhibits a shift in transfer characteristics towards negative gate voltages after the FBS proteins adsorbed on the surface and subsequently the cells were cultivated on top of them. This is a clear sign of a lowered transistor's conductivity. This effect cannot be fully explained solely by the electrostatic field effect. The most important discrepancy here consists in the fact that the major FBS proteins (albumin, fibronectin, vitronectin) as well as cell membranes are negatively charged under physiologic pH. Thus, their presence near the gate of a *p* type transistor should increase the I_{ds} current flowing through the transistor, which is not the case. As was already mentioned, proteins become denatured on a hydrophobic surface and their hydrophobic core sticks to the surface. Consequently, they can modify the initial equilibrium of the conductive layer, which is a result of the equilibrium of chemical potentials of the diamond and the solution (Chakrapani et al., 2007; Maier et al., 2000). A negative shift occurs as a result of the change of the material properties of diamond (i.e. its conductivity), which is in accord with the lowered steepness of the slope of the transfer curve (transconductance). Sometimes observed increase in the SG-FET gate currents indicates that proteins can lower the electronic barrier of the diamond-electrolyte system resulting from the surface C–H dipoles (Rezek, Krátká, Kromka & Kalbacova, 2010) and can therefore simplify the charge transfer across the interface with the solution. The primary FBS monolayer persists on the surface (Rezek, Ukraintsev, Michalíková, Kromka, Zemek & Kalbacova, 2009; Ukraintsev et al., 2009) and cannot be easily removed by common rinsing methods, even when detergents and enzymes are employed. This explains the stability of the shift in the SG-FET transistor's transfer characteristics.

A further negative shift in transfer characteristics was observed after the cultivation of cells on the device. This shift cannot be ascribed to the cells themselves, because it persists even after the cells are removed. Possible reasons for this shift include the fact that osteoblastic cells attach to the surface only in a limited number of spots (the so-called focal adhesion), which cannot cover the whole gate area, and the remaining cells are not in direct contact with the substrate surface (Kalbacova et al., 2009). Moreover, cells on H-diamond do not tend to spread and adhere but they rather form bridges to O-diamond if it is in close proximity (Kalbacova et al., 2008). The adhesion of osteoblasts is then mediated by proteins, i.e. another FBS protein layer exists between the cell and the diamond surface. This is why the most part of a cell membrane is presumably further than the Debye length in the medium, which amounts to < 10 nm due to the presence of salts and other ionic compounds in the cultivation medium. As a result, we deduce that the shift after the cultivation of cells is a result of a change in the adsorbed layer of proteins, which remains on the diamond surface even after rinsing (Rezek, Ukraintsev, Michalíková, Kromka, Zemek & Kalbacova, 2009; Ukraintsev et al., 2009). Cells can actively participate at such changes because osteoblasts continually modify their surrounding environment and subsequently produce their own ECM. Based on the above reasoning, a model of the interface between the channel of the diamond SG-FET and the cell medium containing proteins and cells can be constructed (Rezek, Krátká, Kromka & Kalbacova, 2010). Figure 11 depicts a schematic concept of this model. The model presumes common cell-plating conditions when the cultivation medium contains FBS proteins.

Further research should answer the question concerning the composition of the layers adsorbed on diamond and the possibility of direct electrical detection of the function of cells

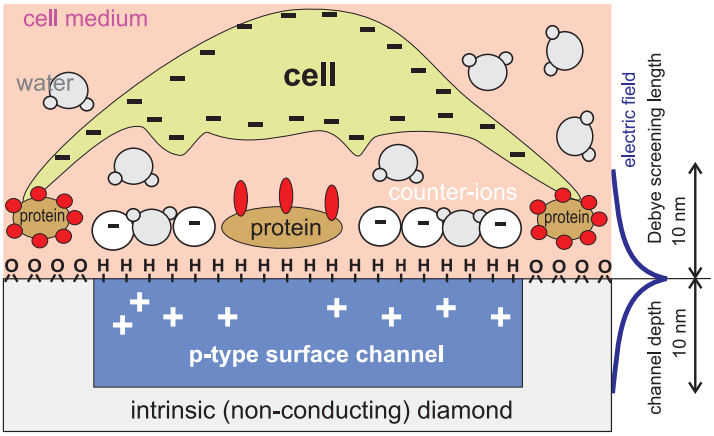

Fig. 11. Schematic sketch of the interface between the surface-condutive SG-FET channel and cell medium containing proteins and cells. The electric field and its reach over the interface is depicted on the right. It demonstrates that the interaction is limited to distances of several tens of nm.

using the interface with diamond, as has already been suggested for neurons (Dankerl et al., 2009).

8. Conclusions

We have demonstrated some of the crucial properties and discussed prospective application of diamond for biomedicine. We showed that nanostructuring of diamond surfaces can be used to tailor adhesion and growth of the cells. We also demonstrated that the combination of oxygen- and hydrogen-terminated surfaces allows for the controlled self-assembly of cells into microstructures. Cells preferably adhere to oxygen-terminated areas, this effect is general and occurs for various types of cells. The best selectivity is achieved for low seeding cell concentrations (2,500 cells cm^2) regardless of the geometry of the surface and usual range of FBS concentrations (5 to 15%). Higher seeding concentrations make it possible for the cells to colonize even the less suitable hydrogen-terminated surface, which is electrically conductive and thus can be utilized in electronic components. Cells plated in the medium without FBS colonize the surface independently of the microstructures. Consequently, the cells' preference stems from the properties of the proteins on H- and O-diamond and it is not a direct consequence of the cells' interaction with diamond surface dipoles. Atomic force microscopy revealed the existence of a thin film (2–4 nm) of proteins on both types of surfaces, however, adopting different conformations on different terminations. Based on these measurements, we propose a model of how the proteins arrange on diamond as a result of the wettability of the surfaces, similarly to other materials. Apart from the protein conformation, other factors, such as the composition and different adhesion of the FBS layer on H- and O-diamond, can contribute the preferential growth of cells.

Electronic effects on the diamond-protein-cell interface were characterized by the SG-FET transistors based on the surface conductivity of nanocrystalline diamond and having the gate insulated solely by hydrogen surface atoms. We show that these transistors are fully

operational and can serve as a transducer (and partly also as an amplifier) of the characteristics of biological material and environment to electrical impulses. Adsorption of proteins from the FBS-enriched cultivation medium and subsequent cultivation of cells on it led to a shift in transfer characteristics of the transistor in the range of as much as a hundred mV. This shift is the result of the adsorption of a thin film of proteins onto the diamond surface as was confirmed by AFM. The key finding here is that these shifts cannot be solely due to electrostatic field effect because the field effect acts in the opposite direction. We propose a model in which the proteins replace the ions close to the diamond surface. The negative shift in the transfer characteristics then results from a change in the material property of diamond (its conductivity), which is in accord with a lowered steepness of the slope (i.e. transconductance) of the measured curves. Related changes in SG-FET gate currents suggest that the FBS layer can block and under certain conditions also promote the transfer of charge across the interface between diamond and the solution. The above findings and conclusions are significant for prospective application of the unique properties of diamond in biosensors and biotechnologies that can be exploited in medicine as well as other fields.

This research was carried out through the financial support of the projects KAN400100701 (AVČR), IAAX00100902 (GAAV), LC510 (MŠMT), LC06040 (MŠMT), MSM0021620806 (MŠMT), 202/09/H041 (GAČR), institutional Research Plan AV0Z10100521, scholarship of J.E. Purkyně Fellowship (BR, AK) and Fellowship 2010 L´Oreal-UNESCO for Women in Science (MK). Zdenka Poláčková, Vlastimil Jurka, Karel Jurek, and Lenka Michalíková are acknowledged for technical support. Software libraries TAFLAB for the measurement software were developed and kindly provided by Dr. Antonín Fejfar.

9. References

Babchenko, O., Kromka, A., Hruska, K., Kalbacova, M., Broz, A. & Vanecek, M. (2009). Fabrication of nano-structured diamond films for saos-2 cell cultivation, *phys. stat. sol. (b)* 206: 2033.

Bajaj, P., Akin, D., Gupta, A., Sherman, D., Shi, B., Auciello, O. & Bashir, R. (2007). Ultrananocrystalline diamond film as an optimal cell interface for biomedical applications, *Biomed. Devices* 9: 787–794.

Browne, M. M., Lubarsky, G. V., Davidson, M. R. & Bradley, R. H. (2004). Protein adsorption onto polystyrene surfaces studied by xps and afm, *Surf. Sci.* 553: 155.

Chakrapani, V., Angus, J. C., Anderson, A. B., Wolter, S. D., Stoner, B. R. & Sumanasekera, G. U. (2007). Charge transfer equilibria between diamond and an aqueous oxygen electrochemical redox couple, *Science* 318: 1424.

Dankerl, M., Eick, S., Hofmann, B., Hauf, M., Ingebrandt, S., Offenhäusser, A., Stutzmann, M. & Garrido, J. A. (2009). Diamond transistor array for extracellular recording from electrogenic cells, *Adv. Funct. Mater.* 19: 2915.

Dankerl, M., Reitinger, A., Stutzmann, M. & Garrido, J. A. (2007). Resolving the controversy on the ph sensitivity of diamond surfaces, *phys. stat. sol. RRL* 2: 31.

Fernandez, J. L. R., Geiger, B., Salomon, D. & Ben-Ze'v, A. (1992). Overexpression of vinculin suppresses cell motility in balb/c 3t3 cells, *Cell. Motil. Cytoskeleton* 22: 127.

Grausova, L., Bacakova, L., Kromka, A., Vanecek, M., Rezek, B. & Lisa, V. (2009). Molecular markers of adhesion, maturation and immune activation of human osteoblast-like MG63 cells on nanocrystalline diamond films, *Diam. Relat. Mater.* 18: 258.

Härtl, A., Schmich, E., Garrido, J. A., Hernando, J., Catharino, S. C. R., Walter, S., Feulner, P., Kromka, A., Steinmüller, D. & Stutzmann, M. (2004). Protein-modified nanocrystalline diamond thin films for biosensor applications, *Nature Mat.* 3: 736.

Kalbacova, M., Kalbac, M., Dunsch, L., Kromka, A., Vanecek, M., Rezek, B., Hempel, U. & Kmoch, S. (2007). The effect of SWCNT and nano-diamond films on human osteoblast cells, *phys. stat. sol. (b)* 244(11): 4356.

Kalbacova, M., Michalíková, L., Barešová, V., Kromka, A., Rezek, B. & Kmoch, S. (2008). Adhesion of osteoblasts on chemically patterned nanocrystalline diamonds, *phys. stat. sol. (b)* 245: 2124.

Kalbacova, M., Rezek, B., Baresova, V., Wolf-Brandstetter, C. & Kromka, A. (2009). Nano-scale topography of nanocrystalline diamonds promotes differentiation of osteoblasts, *Acta Biomaterialia* 5: 3076.

Kalbacova, M., Roessler, S., Hempel, U., Tsaryk, R., Peters, K., Scharnweber, D., Kirkpatrick, C. & Dieter, P. (2007). The effect of electrochemically simulated titanium cathodic corrosion products on ros production and metabolic activity of osteoblasts and monocytes/macrophages, *Biomaterials* 28: 3263–3272.

Kawarada, H. (1996). Hydrogen-terminated diamond surfaces and interfaces, *Surf. Sci. Rep.* 26(7): 205.

Kozak, H., Kromka, A., Babchenko, O. & Rezek, B. (2010). Directly grown nanocrystalline diamond field-effect transistor microstructures, *Sensor Lett.* 8: 482.

Kozak, H., Kromka, A., Ledinský, M. & Rezek, B. (2009). Enhancing nanocrystalline diamond surface conductivity by deposition temperature and chemical post-processing, *phys. stat. sol. (a)* 206: 276.

Kromka, A., Babchenko, O., Izak, T., Hruska, K. & Rezek, B. (2011). Linear antenna microwave plasma cvd deposition of diamond films over large areas, *Vacuum* p. in press.

Kromka, A., Rezek, B., Kalbacova, M., Baresova, V., Zemek, J., Konak, C. & Vanecek, M. (2009). Diamond seeding and growth of hierarchically structured films for tissue engineering, *Adv. Eng. Mater.* 11: B71.

Kromka, A., Rezek, B., Remeš, Z., Michalka, M., Ledinský, M., Zemek, J., Potměšil, J. & Vaněček, M. (2008). Formation of continuous nanocrystalline diamond layer on glass and silicon at low temperatures, *Chem. Vap. Deposition* 14: 181.

Maier, F., Riedel, M., Mantel, B., Ristein, J. & Ley, L. (2000). Origin of surface conductivity in diamond, *Phys. Rev. Lett.* 85: 3472.

Maier, F., Ristein, J. & Ley, L. (2001). Electron affinity of plasma-hydrogenated and chemically oxidized diamond (100) surfaces, *Phys. Rev. B* 64: 65411.

Michalíková, L., Rezek, B., Kromka, A. & Kalbacova, M. (2009). CVD diamond films with hydrophilic micro-patterns for self-organisation of human osteoblasts, *Vacuum* 84: 61.

Nebel, C. E., Rezek, B., Shin, D., Watanabe, H. & Yamamoto, T. (2006). Electronic properties of h-terminated diamond in electrolyte solutions, *J. Appl. Phys.* 99: 033711.

Nebel, C. E., Shin, D., Rezek, B., Tokuda, N., Uetsuka, H. & Watanabe, H. (2007). Diamond and biology, *J. R. Soc. Interface* 4: 439.

Popov, C., Kulisch, W., Reithmaier, J., Dostalova, T., Jelinek, M., Anspach, N. & Hammann, C. (2007). Bioproperties of nanocrystalline diamond/amorphous carbon composite films, *Diamond Relat. Mater.* 16: 735.

Potocky, S., Kromka, A., Potmesil, J., Vorlicek, Z., Vanecek, M. & Michalka, M. (2007). Investigation of nanocrystalline diamond films grown on silicon and glass at substrate temperature below 400°c, *Diamond Relat. Mater.* 16: 744–747.

Rezek, B., Krátká, M., Kromka, A. & Kalbacova, M. (2010). Effects of protein inter-layers on cell-diamond fet characteristics, *Biosens. Bioelectron.* 26: 1307.

Rezek, B., Michalíková, L., Ukraintsev, E., Kromka, A. & Kalbacova, M. (2009). Micro-pattern guided adhesion of osteoblasts on diamond surfaces, *Sensors* 9: 3549.

Rezek, B., Sauerer, C., Nebel, C. E., Stutzmann, M., Ristein, J., Ley, L., Snidero, E. & Bergonzo, P. (2003). Fermi level on hydrogen terminated diamond surfaces, *Appl. Phys. Lett.* 82: 2266.

Rezek, B., Shin, D., Nakamura, T. & Nebel, C. E. (2006). Geometric properties of covalently bonded DNA on single-crystalline diamond, *J. Am. Chem. Soc.* 128: 3884.

Rezek, B., Shin, D., Uetsuka, H. & Nebel, C. E. (2007). Microscopic diagnostics of DNA molecules on mono-crystalline diamond, *phys. stat. sol. (a)* 204: 2888.

Rezek, B., Shin, D., Watanabe, H. & Nebel, C. E. (2007). Intrinsic hydrogen-terminated diamond as ion-sensitive field effect transistor, *Sens. Actuators B* 122: 596.

Rezek, B., Ukraintsev, E., Kromka, A., Ledinský, M., Brož, A., Nosková, L., Hartmannová, H. & Kalbacova, M. (2010). Assembly of osteoblastic cell micro-arrays on diamond guided by protein pre-adsorption, *Diam. Relat. Mater.* 19: 153.

Rezek, B., Ukraintsev, E., Michalíková, L., Kromka, A., Zemek, J. & Kalbacova, M. (2009). Adsorption of fetal bovine serum on H/O-terminated diamond studied by atomic force microscopy, *Diam. Relat. Mater.* 18: 918.

Ri, S. G., Mizumasa, T., Akiba, Y., Hirose, Y., Kurosu, T. & Iida, M. (1995). Formation mechanism of p-type surface conductive layer on deposited diamond films, *Jpn. J. Appl. Phys.* 34: 5550.

Shakenraad, J. & Busscher, H. (1989). Cell-polymer interactions:the influence of protein adsorption, *Colloid Surf.* 42: 331–343.

Tanaka, M., Takayama, A., Ito, E., Sunami, H., Yamamoto, S. & Shimomura, M. (2007). Effect of pore size of self-organized honeycomb-patterned polymer films on spreading, focal adhesion, proliferation, and function of endothelial cells, *J. Nanosci. Nanotechnol.* 7: 763–772.

Tang, L., Tsai, C., Gerberich, W., Kruckeberg, L. & Kania, D. (1995). Biocompatibility of chemical-vapour-deposited diamond, *Biomaterials* 16(6): 483–488.

Tsugawa, K., Ishihara, M., Kim, J., Koga, Y. & Hasegawa, M. (2010). Nanocrystalline diamond film growth on plastic substrates at temperatures below 100°c from low-temperature plasma, *Phys. Rev. B* 82: 125460.

Ukraintsev, E., Rezek, B., Kromka, A., Broz, A. & Kalbacova, M. (2009). Long-term adsorption of fetal bovine serum on H/O-terminated diamond studied in-situ by atomic force microscopy, *phys. stat. sol. (b)* 246: 2832.

Yang, W., Auciello, O., Butler, J. E., Cai, W., Carlisle, J. A., Gerbi, J. E., Gruen, D. M., Knickerbocker, T., Lasseter, T. L., J. N. Russel, J., Smith, L. M. & Hamers, R. J. (2002). DNA-modified nanocrystalline diamond thin films as stable, biologically active substrates, *Nature Mat.* 1: 253.

Zhao, G., Zinger, O., Schwartz, Z., Wieland, M., Landolt, D. & Boyan, B. D. (2006). Osteoblast-like cells are sensitive to submicron-scale surface structure, *Clin. Oral. Implant. Res.* 17: 258.

New Perspectives in Biosensors Technology and Applications

Edited by Prof. Pier Andrea Serra

ISBN 978-953-307-448-1
Hard cover, 448 pages
Publisher InTech
Published online 24, June, 2011
Published in print edition June, 2011

A biosensor is a detecting device that combines a transducer with a biologically sensitive and selective component. Biosensors can measure compounds present in the environment, chemical processes, food and human body at low cost if compared with traditional analytical techniques. This book covers a wide range of aspects and issues related to biosensor technology, bringing together researchers from 12 different countries. The book consists of 20 chapters written by 69 authors and divided in three sections: Biosensors Technology and Materials, Biosensors for Health and Biosensors for Environment and Biosecurity.

INTECH
open science | open minds

InTech Europe
University Campus STeP Ri
Slavka Krautzeka 83/A
51000 Rijeka, Croatia
Phone: +385 (51) 770 447
Fax: +385 (51) 686 166
www.intechopen.com

InTech China
Unit 405, Office Block, Hotel Equatorial Shanghai
No.65, Yan An Road (West), Shanghai, 200040, China
中国上海市延安西路65号上海国际贵都大饭店办公楼405单元
Phone: +86-21-62489820
Fax: +86-21-62489821